A conserved late endosome–targeting signal required for Doa4 deubiquitylating enzyme function

Alexander Amerik,[1] Nazia Sindhi,[1] and Mark Hochstrasser[2]

[1]Department of Pharmacology, University of Connecticut Health Center, Farmington, CT 06030
[2]Department of Molecular Biophysics and Biochemistry, Yale University, New Haven, CT 06520

Enzyme specificity in vivo is often controlled by subcellular localization. Yeast Doa4, a deubiquitylating enzyme (DUB), removes ubiquitin from membrane proteins destined for vacuolar degradation. Doa4 is recruited to the late endosome after ESCRT-III (endosomal sorting complex required for transport III) has assembled there. We show that an N-terminal segment of Doa4 is sufficient for endosome association. This domain bears four conserved elements (boxes A–D). Deletion of the most conserved of these, A or B, prevents Doa4 endosomal localization. These mutants cannot sustain ubiquitin-dependent proteolysis even though neither motif is essential for deubiquitylating activity. Ubiquitin-specific processing protease 5 (Ubp5), the closest paralogue of Doa4, has no functional overlap. Ubp5 concentrates at the bud neck; its N-terminal domain is critical for this. Importantly, substitution of the Ubp5 N-terminal domain with that of Doa4 relocalizes the Ubp5 enzyme to endosomes and provides Doa4 function. This is the first demonstration of a physiologically important DUB subcellular localization signal and provides a striking example of the functional diversification of DUB paralogues by the evolution of alternative spatial signals.

Introduction

In eukaryotic cells, most short-lived proteins are degraded by the ubiquitin system (Hochstrasser, 1996; Hershko and Ciechanover, 1998; Weissman, 2001). Modification of cellular proteins with Lys48-linked polyubiquitin chains leads to their degradation by the 26S proteasome. Ubiquitylation also participates in the down-regulation of plasma membrane proteins, including many receptors and transporters. In this case, the targeted proteins are modified by either a single ubiquitin or short Lys63-linked ubiquitin oligomers (Galan and Haguenauer-Tsapis, 1997; Hicke and Dunn, 2003). These modifications do not target substrate molecules to the proteasome. Instead, they promote endocytosis of the tagged membrane proteins and their trafficking to the lysosome (equivalent to the yeast vacuole). Ubiquitin-modified proteins first sort to the limiting membrane of the late endosome, which invaginates at multiple sites, leading to the accumulation of internal vesicles. The membrane proteins accumulate in these vesicles, but ubiquitin does not. The mature late endosome structure is called a multivesicular body (MVB), which then fuses with the lysosome, resulting in breakdown of the internal vesicles by lysosomal lipases and proteases (Dupre et al., 2001; Hicke and Dunn, 2003).

Ubiquitin is a relatively stable protein in yeast despite its covalent linkage to many proteins destined for proteasomal or vacuolar degradation (Swaminathan et al., 1999). This is possible because ubiquitin-protein modification is transient. Deubiquitylating enzymes (DUBs) release ubiquitin from polyubiquitin conjugates by cleaving the isopeptide bond between the ubiquitins in a chain or at the ubiquitin C terminus linked to substrate. The yeast DUB family consists of at least 20 members, including 16 in the ubiquitin-specific processing protease (UBP) subfamily (Amerik et al., 2000b; Verma et al., 2002; Amerik and Hochstrasser, 2004).

Mechanisms regulating DUB activity in the cell are only beginning to be analyzed. Subcellular localization, posttranslational modification, and interaction with regulatory factors are all likely to play important roles in DUB regulation (Nijman et al., 2005). For instance, several DUBs associate with the 26S proteasome, and this association is required for full activity. Rpn11/POH1, a DUB of the MPN^+/JAMM class, is an integral subunit of the proteasome 19S regulatory complex (Verma et al., 2002; Yao and Cohen, 2002). Its deubiquitylating activity

Correspondence to Alexander Amerik: amerik@uchc.edu; or Mark Hochstrasser: mark.hochstrasser@yale.edu

Abbreviations used in this paper: CPS, carboxypeptidase S; DUB, deubiquitylating enzyme; ESCRT, endosomal sorting complex required for transport; HAUSP, herpesvirus-associated ubiquitin-specific protease; IsoT, isopeptidase T; LEL, late endosome localization; MVB, multivesicular body; pCPS, CPS precursor; RHD, rhodanese homology domain; UBP, ubiquitin-specific processing protease; VPS, vacuolar protein sorting.

The online version of this article contains supplemental material.

The Journal of Cell Biology, Vol. 175, No. 5, December 4, 2006 825–835
http://www.jcb.org/cgi/doi/10.1083/jcb.200605134

requires interaction with other subunits of the 19S complex. Ubp6 binds to the 19S subunit Rpn1, and this interaction strongly stimulates Ubp6 enzymatic activity (Leggett et al., 2002). Thus, the activities of both Rpn11 and Ubp6 are delimited to their desired site of action, the proteasome. Other DUBs may not need to be regulated in this manner because they have intrinsically high substrate specificity. For instance, isopeptidase T (IsoT) and its yeast orthologue Ubp14 regenerate free ubiquitin from unanchored polyubiquitin chains, but no activity is seen toward polyubiquitin-protein conjugates (Wilkinson et al., 1995; Amerik et al., 1997). This specificity was traced to an IsoT/Ubp14 element called the ZnF-UBP or DAUP domain (Amerik et al., 2000a), which is necessary for ubiquitin binding and forms a pocket around the free C-terminal tail of the ubiquitin chain (Reyes-Turcu et al., 2006).

Doa4, a 926-residue yeast DUB of the UBP class, contributes to the release of ubiquitin from ubiquitin-protein conjugates destined for degradation (Papa and Hochstrasser, 1993; Papa et al., 1999; Amerik et al., 2000a; Amerik and Hochstrasser, 2004). The enzyme acts primarily at the late endosome membrane, although genetic and biochemical data suggest that it may have additional roles linked to the proteasome (Papa et al., 1999; Swaminathan et al., 1999). The inactivation of Doa4 leads to severe phenotypic abnormalities, including the depletion of free ubiquitin, accumulation of apparent proteolytic remnants attached to short ubiquitin chains, defects in the proteolysis of both proteasomal and vacuolar substrates, hypersensitivity to amino acid analogues such as canavanine, and a strong sporulation defect.

Multiple observations indicate that Doa4 is responsible for deubiquitylating membrane proteins at the MVB. First, *doa4* mutations interact genetically with mutations in class E vacuolar protein-sorting (VPS) factors, which are essential for maturation of the late endosome into MVBs (Amerik et al., 2000b). Inactivation of these factors compromises MVB vesiculation, leading to the accumulation of stacked membrane cisternae known as the class E compartment (Rieder et al., 1996), and causes strong suppression of the phenotypic abnormalities associated with *doa4* mutations. Second, Doa4 colocalizes with components of the large MVB-localized endosomal sorting complex required for transport III (ESCRT-III; Babst et al., 2002). Specifically, in yeast cells lacking the AAA ATPase Vps4, Doa4 accumulates in the class E compartment along with the ESCRT-III factors Vps24/Did3 and Snf7/Vps32/Did1 (Amerik et al., 2000b). Third, transmembrane proteins in transit to the vacuole from either the cell surface or the Golgi accumulate in ubiquitinated forms in *doa4* cells (Dupre et al., 2001; Katzmann et al., 2001). Finally, Doa4 is able to bind to the class E VPS protein Bro1, which associates directly with the Snf7 subunit of ESCRT-III; Bro1 may help recruit Doa4 to the late endosome (Luhtala and Odorizzi, 2004).

Both endocytic and biosynthetic cargoes need to be ubiquitylated in order to be transported efficiently to the vacuolar interior. However, Doa4 must remove the ubiquitin tag before or during cargo protein movement into the internal vesicles of the MVB to prevent ubiquitin from getting degraded along with the conjugated cargo protein. Therefore, Doa4 enzyme activity needs to be tightly controlled. In this study, we demonstrate that binding to the late endosome plays an important role in regulating Doa4 function. The N-terminal region of Doa4 is both necessary and sufficient for this binding. We identified four short conserved sequence blocks within this domain. From a deletion analysis of two of these motifs (boxes A and B), we determined that although these elements have no role in Doa4 expression or catalytic activity, they are critical for its physiological function. Deletion of either box A or B causes a phenotype equivalent to a complete loss of Doa4, and this correlates with the inability of the mutant proteins to interact with the late endosome. Notably, an N-terminal fragment of Ubp5, another yeast DUB, directs Ubp5 to the yeast bud neck, but when this segment is replaced with an N-terminal fragment of Doa4, the chimera relocalizes to the late endosome, where it can partially substitute for Doa4. These data show that the N-terminal extensions of Doa4 and Ubp5 determine their respective cellular distributions and that this contributes to the functional specialization of these paralogues.

Results

An N-terminal segment of Doa4 allows interaction with the late endosome

Several normally soluble ESCRT-III factors, including Snf7 (Vps32/Did1) and Vps24 (Did3), concentrate in the class E compartment in yeast mutants with a defective Vps4 ATPase (Babst et al., 1998). A Doa4-GFP fusion protein, which is primarily cytosolic in wild-type cells, also concentrates in several spots (usually from one to three per cell) adjacent to the vacuole (Amerik et al., 2000b). Colocalization of Doa4-GFP and Vps24-HA by indirect immunofluorescence in *vps4Δ* cells suggested that these spots were class E compartments, but low cellular levels of Doa4-GFP made the detection of foci difficult. To enhance detection sensitivity and to verify the colocalization of endogenous Doa4 with ESCRT-III, we constructed wild-type and *vps4* strains expressing Doa4 tagged with nine c-myc epitopes. Cells were costained with antibodies against endogenous Snf7 and c-myc. Despite the low cellular concentration of Doa4, bright foci were detected with the anti-myc antibody in *vps4Δ* cells, and these foci did indeed coincide with those of the ESCRT-III subunit Snf7 adjacent to vacuoles (Fig. 1 A).

The UBP subfamily of DUBs, to which Doa4 belongs, comprises a diverse set of cysteine proteases with two well-conserved motifs, the Cys and His boxes, which include all of the active site residues (Hu et al., 2002; Amerik and Hochstrasser, 2004). Many UBPs have long N-terminal segments (and occasionally C-terminal ones) that extend from the core catalytic domain but are of generally unknown function. These extensions may have regulatory roles. In a well-studied example, the N-terminal domain of the human UBP called herpesvirus-associated ubiquitin-specific protease ([HAUSP] USP7) binds the p53 tumor suppressor, allowing HAUSP to cleave polyubiquitin-p53 conjugates and, thereby, limit p53 degradation (Li et al., 2002). Previously, we had shown that the N-terminal noncatalytic region of Doa4 (~560 residues) conferred Doa4 function

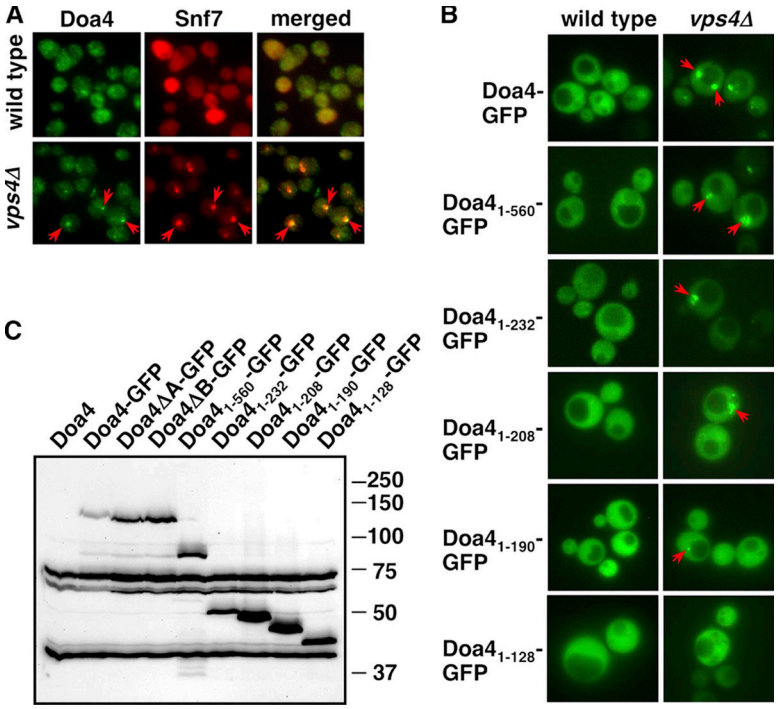

Figure 1. **The N-terminal domain of Doa4 is sufficient for association with the late endosome.** (A) Doa4-myc$_9$ and Snf7 accumulate in an aberrant late endosome (the class E compartment; arrows in A and B) in a *vps4* mutant. Cells were costained with antibodies to myc and Snf7. (B) Localization by GFP fluorescence of truncated Doa4-GFP fusion proteins in wild-type and *vps4Δ* cells. (C) Expression of the Doa4-GFP derivatives measured by anti-GFP immunoblot analysis.

on the catalytic domain of Ubp5, as did a shorter, 310-residue N-terminal Doa4 fragment (Papa et al., 1999).

We hypothesized that the N-terminal noncatalytic domain of Doa4 might target the enzyme to the late endosome membrane. To test this model, we expressed C-terminally truncated versions of Doa4 fused to GFP in wild-type and *vps4* mutant cells and examined their cellular localization (Fig. 1 B). Anti-GFP immunoblot analysis showed proteins of the expected sizes that were expressed at levels similar to or slightly above that of the full-length Doa4-GFP fusion protein (Fig. 1 C). The Doa4$_{1–208}$-, Doa4$_{1–232}$-, and Doa4$_{1–560}$-GFP fusion proteins were all concentrated at the class E compartment in a *vps4Δ* strain (Fig. 1 B and Fig. S1, available at http://www.jcb.org/cgi/content/full/jcb.200605134/DC1). In *vps4Δ* cells transformed with the Doa4$_{1–190}$-GFP derivative, Doa4 foci were still observed, but they were smaller than those of the aforementioned fusions. In contrast, localization of Doa4$_{1–128}$-GFP to the late endosome was not observed. The modest differences in mutant protein expression levels did not correlate with class E localization. Collectively, the deletion analysis demonstrated that the first 208 residues of Doa4 are sufficient for its endosomal localization, whereas residues between 129 and 208 are necessary for the interaction. We named the N-terminal 208-residue segment the late endosome localization (LEL) domain or signal.

Conserved sequence motifs in the LEL domain

We previously isolated the *Kluyveromyces lactis DOA4* orthologue by virtue of its ability to suppress the phenotype of a *Saccharomyces cerevisiae doa4* mutant (Amerik et al., 2000a). Overall, the *K. lactis* enzyme is 43% identical to its *S. cerevisiae* counterpart. The catalytic domains are the most closely related (64% identity). Several other potential Doa4 orthologues have been identified recently. These include potential ORFs from *Saccharomyces bayanus* (86% identity), *Saccharomyces mikatae* (88% identity), and *Eremothecium gossypii* (46% identity; Fig. 2). Doa4 is also 41% identical to the Ubp5 paralogue, but, surprisingly, we could detect no functional overlap between these two enzymes even when the latter was expressed from a high copy plasmid (Papa et al., 1999).

The LEL domain of Doa4 includes four short motifs that are well conserved among the Doa4 orthologues. We named these boxes A, B, C, and D (Fig. 2). In contrast, Ubp5 has diverged substantially in these regions. For instance, in box A, there is a negatively charged Glu at the fourth position, where there is a positively charged Lys in all of the Doa4 orthologues (and an uncharged Gln in the potential orthologue from *E. gossypii*); a bulky aliphatic at the sixth position but an Ala in Ubp5; an Asp at the seventh position versus Glu in Ubp5; and a Leu at the ninth residue, where there is a Trp in Ubp5. The potential significance of box D for endosomal localization is suggested by the impaired capacity of Doa4$_{1–190}$-GFP, which lacks box D, to concentrate at the class E compartment (Fig. 1 B). To address the functional relevance of these motifs more fully, we undertook a detailed analysis of alleles bearing deletions of the two most conserved ones, boxes A and B.

Doa4 lacking box A or B is nonfunctional in vivo

Mutant *doa4* alleles with precise deletions of box A (residues 51–63) or B (residues 94–100) were generated in the pDOA4-GFP plasmid backbone, yielding pDOA4ΔA- and pDOA4ΔB-GFP. The plasmids were transformed into a *doa4Δ* strain, and expression of the mutant proteins at or above wild-type levels was confirmed by anti-GFP immunoblot analysis (Fig. 1 B). The *doa4ΔA* and *doa4ΔB* mutants were tested by multiple assays.

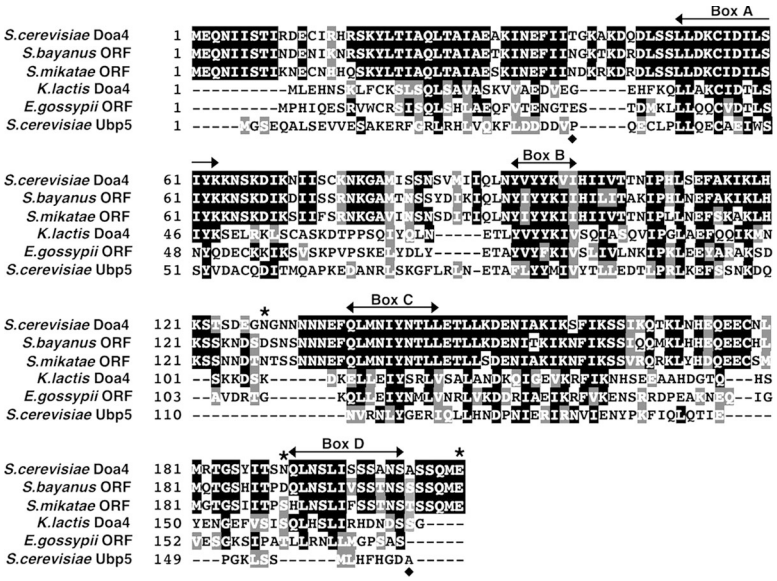

Figure 2. **Sequence alignments of the N-terminal domains of Doa4 and related proteins.** *S. cerevisiae* Doa4 (Z74365), *S. bayanus* potential ORF 21201, *S. mikatae* potential ORF 3452, *K. lactis* Doa4 (AF303215), *E. gossypii* potential ORF (Q754R5), and *S. cerevisiae* Ubp5 (P39944). Conserved boxes A–D are indicated. Deletion endpoints at Asn128, Asn190, and Glu208 in *S. cerevisiae* Doa4 are marked by asterisks, and those at Pro35 and Ala162 of Ubp5 are indicated by diamonds.

Although wild-type MHY501 cells can survive exposure to the arginine analogue canavanine at concentrations up to 1.5 μg/ml, a *doa4Δ* mutant (MHY623) cannot form colonies even at canavanine levels as low as 0.4 μg/ml. As expected, the wild-type Doa4-GFP fusion protein completely suppressed the canavanine sensitivity of the *doa4Δ* mutant. Neither the *ΔA* nor *ΔB* alleles allowed survival on plates with 0.4 μg/ml canavanine (Fig. 3 A).

Another prominent feature of the *doa4Δ* mutant is the accumulation of small ubiquitin-containing species, which appear to be proteolytic remnants attached to short ubiquitin chains, and strongly reduced levels of free ubiquitin (Papa and Hochstrasser, 1993; Papa et al., 1999). The *ΔA* and *ΔB* alleles also could not suppress these aberrations and, in fact, caused a further increase in levels of the short-chain species (Fig. 3 B). This dominant-negative effect might reflect an interaction of the Doa4 mutants with a protein that binds both Doa4 and another DUB that normally is able to compensate weakly for Doa4 loss.

To examine the role of boxes A and B in Doa4-dependent proteolysis, we used pulse-chase analysis to measure degradation rates of three well-characterized ubiquitin system substrates in the *doa4ΔA* and *doa4ΔB* strains. We used two model test substrates, Ub-P–β-galactosidase and L–β-galactosidase, and the naturally short-lived transcription factor Matα2. Degradation of all three substrates was severely impaired in both mutants (Fig. 4).

Deubiquitylation at the endosome membrane requires Doa4 boxes A and B

Monoubiquitin addition to transmembrane biosynthetic cargo destined for the vacuole lumen serves as a signal for cargo sorting to the invaginating vesicles of MVBs; Doa4 is responsible for removing ubiquitin before cargo internalization into MVB vesicles (Katzmann et al., 2002). A model substrate for this is the vacuolar hydrolase carboxypeptidase S (CPS), which is synthesized as an integral membrane protein. In the vacuole, the CPS precursor (pCPS) is cleaved from its transmembrane anchor by resident hydrolases to yield the mature lumenal form (Spormann et al., 1992). Doa4 removes the ubiquitin tag from pCPS at the late endosome (Katzmann et al., 2001). We investigated the contribution of Doa4 boxes A and B to this process.

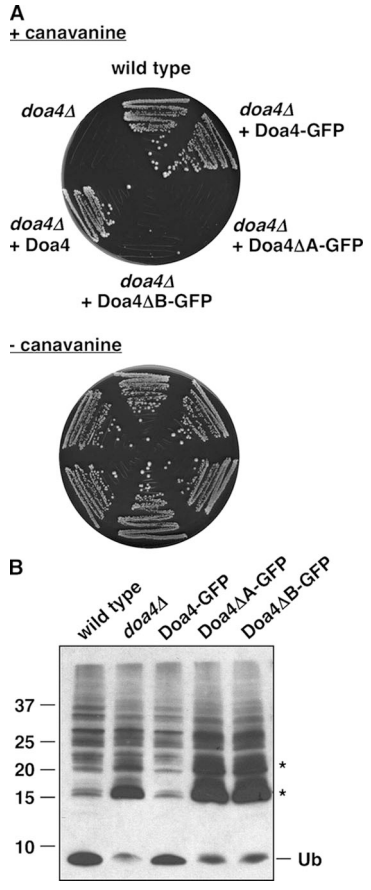

Figure 3. **Deletion of box A or B in Doa4 abrogates function.** (A) Mutant *doa4Δ* cells transformed with plasmids encoding the indicated proteins were grown on 0.4 μg/ml canavanine sulfate or control plates. (B) Anti-ubiquitin immunoblot analysis of the *doa4Δ* mutant transformed with the pDOA4-GFP plasmid or its ΔA or ΔB derivatives. Ubiquitin-peptide conjugates are marked with asterisks.

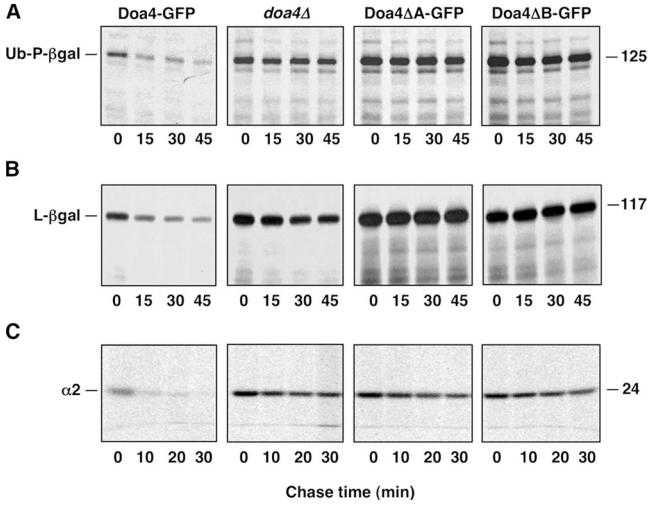

Figure 4. **The *doa4* ΔA and ΔB mutants are defective in proteolysis by the ubiquitin–proteasome pathway.** (A–C) The substrates Ub-P–β-galactosidase (A), L–β-galactosidase (B), and α2 (C) were assayed by pulse-chase analysis in *doa4Δ* cells transformed with empty vector, pDOA4-GFP, or the ΔA or ΔB derivatives. Degradation of endogenous α2 was analyzed, whereas Ub-P–β-galactosidase and L–β-galactosidase were expressed from plasmid-borne *GAL*-driven alleles induced with galactose.

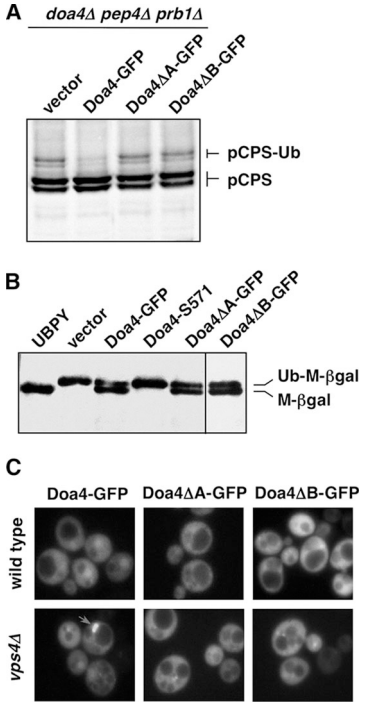

Figure 5. **Phenotype of the *doa4* ΔA and ΔB mutants.** (A) Monoubiquitylated CPS precursor (pCPS) accumulates in the *doa4* ΔA and ΔB mutants. Anti-CPS immunoblot analysis was performed on yeast *doa4Δ pep4Δ prb1Δ* cells expressing the indicated proteins. The pCPS-containing bands appear as doublets because pCPS is modified with one or two N-linked core oligosaccharides during its biogenesis (Spormann et al., 1992). (B) Deletion of boxes A and B does not affect the enzymatic activity of Doa4. Doa4ΔA- and Doa4ΔB-GFP mutants were coexpressed with a ubiquitin-M–β-galactosidase fusion protein in *E. coli*. Mammalian UBPY and the catalytically inactive Doa4-S571 mutant served as positive and negative controls, respectively. Extracts were analyzed by anti–β-galactosidase immunoblotting. (C) Deletion of boxes A and B prevent the relocalization of Doa4 to the class E compartment in *vps4* cells. Arrow marks a class E compartment.

Anti-CPS immunoblot analysis was performed in transformants of a *doa4 pep4 prb1* mutant (Fig. 5 A). Inactivation of the Pep4 and Prb1 vacuolar proteases blocks virtually all vacuolar proteolysis, including the cleavage of pCPS, and allows the detection of ubiquitylated proteins that enter the vacuole. Monoubiquitylated pCPS (pCPS-Ub) accumulated in cells lacking Doa4 as expected (Fig. 5 A, first lane), and this was suppressed by pDOA4-GFP (Fig. 5 A, second lane). In contrast, neither pDOA4ΔA- nor pDOA4ΔB-GFP was able to suppress the accumulation of pCPS-Ub (Fig. 5 A, third and fourth lanes). We conclude that boxes A and B are required for the Doa4-mediated deubiquitylation of protein cargo in the MVB.

The failure of the box A/B mutants to deubiquitylate pCPS was not caused by a defect in Doa4 catalytic activity. Mutant versions of Doa4 were expressed in *Escherichia coli* along with the ubiquitin fusion substrate Ub-M–β-galactosidase (Fig. 5 B). Cleavage of ubiquitin from M–β-galactosidase by the mutants was indistinguishable from wild-type Doa4 in this assay. Therefore, these short N-terminal deletions are unlikely to have disrupted overall Doa4 folding or catalytic activity and must instead impair some other feature of Doa4 function in the cell.

Boxes A and B are the most conserved elements in the LEL domain, which targets Doa4 to the late endosome (Fig. 1 B), so we tested whether these elements are necessary for this localization function. Indeed, both Doa4ΔA- and Doa4ΔB-GFP failed to concentrate in the class E compartment in *vps4* cells (Fig. 5 C). Therefore, boxes A and B are required for Doa4 association with the late endosome.

The Doa4 LEL signal redirects Ubp5 to the late endosome

As noted above, *S. cerevisiae* has an enzyme, Ubp5, that is much more closely related to Doa4 than any other DUB in this species. The similarity between Doa4 and Ubp5 extends over most of their lengths, including the more divergent N-terminal domains (Papa et al., 1999). However, no functional overlap between the two proteins has been detected. Potentially, this separation of function could derive, at least in part, from the segregation of Doa4 and Ubp5 to different cellular compartments. The cellular distribution of Ubp5 has not been reported. Therefore, we tagged Ubp5 with GFP and examined its localization by intrinsic GFP fluorescence. The protein was seen throughout the cytoplasm and nucleus, but a fraction concentrated at the bud neck and incipient bud sites (Fig. 6, A and B).

Given that Ubp5 and Doa4 are most diverged in their N termini and that the LEL signal in Doa4 is in its N-terminal extension, we asked whether the distinct localization of Ubp5 was also caused by determinants in its N-terminal region. Residues 1–35 of Ubp5 have little obvious similarity to Doa4, whereas residues 36–162, which align with the LEL region of Doa4, have diverged in the regions corresponding to boxes A– D (Fig. 2). Like full-length Ubp5-GFP, a fraction of $Ubp5_{\Delta 2–35}$-GFP localized to the bud neck in dividing yeast cells, but the $Ubp5_{\Delta 2–162}$-GFP derivative no longer concentrated there (Fig. 6 A). These results suggest that sequences within the Ubp5 segment

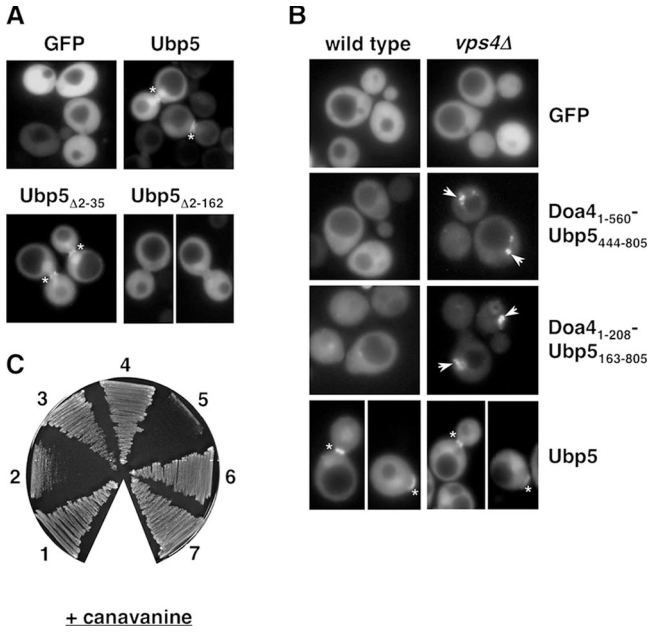

Figure 6. **Substitution of the Ubp5 N-terminal domain with the Doa4 LEL (residues 1–208) relocalizes the Ubp5 enzyme from the bud neck to endosomes and provides Doa4 function.** (A) Cellular distribution of Ubp5-GFP and N-terminal deletion mutants. (B) Localization of Doa4-Ubp5-GFP chimeras in wild-type and *vps4* cells. (A and B) Bud neck and bud sites are marked by asterisks, and the class E compartment is indicated by arrows. (C) Growth of different Doa4-Ubp5 chimeras on 0.4 μg/ml canavanine; growth of all strains on control plates is equal (not depicted). 1, wild-type cells; 2–7, *doa4Δ* cells expressing $Doa4_{1–208}$-$Ubp5_{163–805}$-GFP (2), $Doa4_{1–310}$-$Ubp5_{265–805}$-HA (3), $Doa4_{1–560}$-$Ubp5_{444–805}$-HA (4), vector (5), Doa4 (6), and Doa4-GFP (7).

from residues 36 to 162 are necessary for the bud neck localization of Ubp5.

We determined whether the N-terminal domain of Doa4 could redirect Ubp5 to the late endosome and, if so, whether this correlated with any ability to provide Doa4 function. Two chimeras were constructed: one with the Doa4 LEL domain (residues 1–208) replacing the corresponding region of the Ubp5 backbone ($Doa4_{1–208}$-$Ubp5_{163–805}$-GFP) and the other with the full Doa4 extension placed upstream of the Ubp5 catalytic domain ($Doa4_{1–560}$-$Ubp5_{444–805}$-GFP). Both fusions showed predominantly class E compartment localization in *vps4Δ* cells (Fig. 6 B). Interestingly, the LEL domain of Doa4 fused to Ubp5 provided partial Doa4 activity; $Doa4_{1–208}Ubp5_{163–805}$-GFP was able to suppress, albeit incompletely, the hypersensitivity of the *doa4Δ* strain to canavanine (Fig. 6 C, sectors 2 and 5). $Ubp5_{Δ2–162}$-GFP, which lacks the Doa4 LEL signal, does not localize to the late endosome (unpublished data). Thus, the N-terminal domains determine the cellular localization of Doa4 and Ubp5, and the LEL signal of Doa4 can confer Doa4 function on a distinct DUB.

Loss of Bro1 leads to a *doa4*-like phenotype

Endosomal localization of Doa4, as determined by trapping of the protein in the class E compartment in *vps4* mutants, requires the ESCRT-III components Snf7 and Vps24 (Amerik et al., 2000b). In another strain background, Snf7 was also found to be necessary for such Doa4 localization but Vps24 was not (Luhtala and Odorizzi, 2004). At the same time, the latter study implicated another class E VPS factor, Bro1, in recruiting Doa4 to the endosome membrane, and the overexpression of Doa4 rescued defects associated with a *bro1* mutation. Mutations in Bro1 cause accumulation of the class E compartment and mislocalization of protein cargo there (Odorizzi et al., 2003). Bro1 itself accumulates in the class E compartment in cells defective for the Vps4 ATPase.

Given that previous studies had already yielded some apparent differences between VPS factor requirements for Doa4 localization to the endosomes (Amerik et al., 2000b; Luhtala and Odorizzi, 2004), we examined the function of Bro1 in more detail. First, we analyzed free ubiquitin and ubiquitin-conjugate profiles in cells deleted for the *BRO1* gene. Strikingly, a *doa4*-like depletion of free ubiquitin and accumulation of small ubiquitin-containing species was observed in the *bro1Δ* mutant (Fig. 7 A). Inactivation of Vps4 efficiently suppresses the phenotypic abnormalities of *doa4Δ* cells (Amerik et al., 2000b). Similarly, strong suppression of the aberrant ubiquitin profile of *bro1Δ* was seen in a *bro1Δ vps4Δ* double mutant (Fig. 7 A). These data are consistent with a close link between Bro1 and Doa4 function.

If Bro1 were necessary for recruiting Doa4 to the late endosome, *bro1Δ vps4Δ* cells should no longer concentrate Doa4-GFP in the class E compartment, as reported previously (Luhtala and Odorizzi, 2004). Unexpectedly, we found that the presence or absence of Bro1 did not appear to alter the ability of Doa4-GFP to localize to the class E compartment in *vps4Δ* cells (Fig. 7 B and Fig. S2, available at http://www.jcb.org/cgi/content/full/jcb.200605134/DC1). These data suggested that yeast might have more than one Doa4 receptor for the endosome, although Doa4 function in the MVB pathway appears to require Bro1 (because the loss of Bro1 mimicked the loss of Doa4 phenotypically). Conceivably, an alternative Doa4 receptor or cofactor with lower affinity for Doa4 might partially substitute for Bro1 when Doa4 levels are elevated, as when Doa4-GFP is expressed from a multicopy plasmid (Fig. 7 B). The overexpression of Doa4 did appear to suppress, albeit only very weakly, the *bro1Δ* defect observed by antiubiquitin blotting (Fig. 7 C).

The strain background used here differed from that used in the earlier Bro1 study (Luhtala and Odorizzi, 2004), which might also contribute to the differences in genetic requirements for Doa4 localization at the late endosome. We note several other differences. In the Luhtala and Odorizzi (2004) wild-type strain, CPS localizes exclusively within the vacuolar lumen, but in our background, a considerable fraction of CPS is found at the vacuolar membrane in wild-type cells (unpublished data). In addition, Bro1 did not cofractionate with either soluble or membrane-bound forms of Doa4 (see Discussion), and we failed to detect a two-hybrid interaction between two proteins (unpublished data).

Discussion

Ubiquitin-modified proteins need to be deubiquitylated in a regulated manner to ensure that the signaling function of

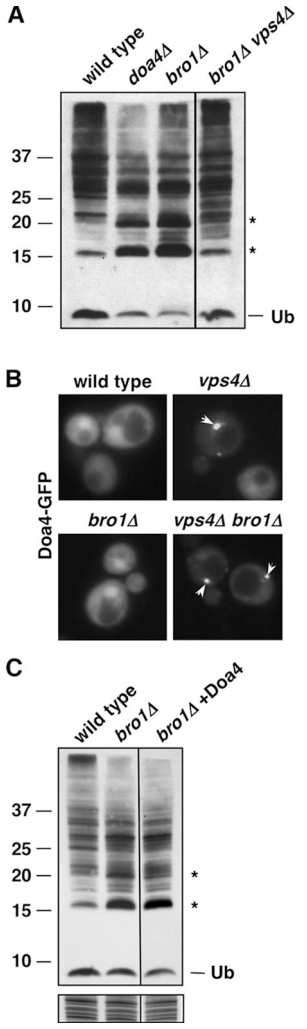

Figure 7. **Functional link between Bro1 and Doa4.** (A) The *bro1Δ* mutant has *doa4Δ*-like ubiquitin homeostasis defects: the accumulation of small ubiquitin-containing species (asterisks) and the depletion of free ubiquitin (Ub) in *bro1Δ* cells (antiubiquitin immunoblot). (B) Bro1 is not essential for Doa4 localization to the class E compartment in *vps4Δ* cells. Arrows mark class E compartments. (C) Overexpression of Doa4 weakly suppresses the accumulation of small ubiquitin-containing species in *bro1Δ* cells. Asterisks mark presumptive ubiquitin-peptide conjugates. The bottom panel shows a section of a Coomassie-stained gel to show protein loading.

ubiquitin is not abrogated prematurely. On the other hand, deubiquitylation of target proteins may be required to switch them to distinct physiological states, and it is also needed to maintain sufficient levels of active, free ubiquitin in the cell. For instance, ubiquitin attachment to a cell surface receptor is a signal for its endocytosis, but if Doa4 were to remove the ubiquitin while the protein was still at the plasma membrane, the endocytic signal would be short circuited. Doa4 appears to only be recruited to ubiquitylated membrane proteins after they have reached the late endosome (or it may only be activated once there), where it cleaves off the ubiquitin moieties before membrane vesiculation into the MVB. This allows the recovery of ubiquitin and might also serve as a signal for other trafficking steps.

The present structure-function study of the Doa4 DUB has demonstrated that an N-terminal segment of its noncatalytic domain is both necessary and sufficient for directing Doa4 to the late endosome. The LEL signal is also able to redirect a functionally distinct yeast DUB, Ubp5, to the late endosomal membrane, allowing partial recovery of Doa4 function. The Ubp5 N-terminal domain normally localizes Ubp5 to the bud neck and incipient bud sites. Thus, the noncatalytic domains of these enzymes restrict them to distinct cellular sites, helping to define their functional specificity.

Restricting DUB activity to specific cellular sites

As outlined in the Introduction, Doa4 functions at the late endosome. There, it removes ubiquitin from both endocytosed membrane proteins and membrane protein cargoes en route from the trans-Golgi network to the vacuole. Certain endocytic factors are also monoubiquitinated (Hicke and Dunn, 2003), and it is possible that Doa4 contributes to their deubiquitylation as well. A key question has been how Doa4 is recruited to the late endosome.

In this study, we have shown that the first 208 residues of Doa4 are sufficient for localization to the class E compartment in *vps4* cells, indicating that this region functions as a LEL signal. Within the LEL domain, four short elements, boxes A–D, are conserved among Doa4 orthologues but have diverged in the *S. cerevisiae* paralogue Ubp5. Deletion analysis indicates that box D contributes to, and boxes A and B are essential for, LEL function. The failure of $Doa4_{1–128}$-GFP to localize to the class E compartment also suggests that box C is required. Consistent with its divergence from Doa4 in the region corresponding to the LEL domain, Ubp5 does not localize to the late endosome. Instead, the N-terminal domain of Ubp5 functions in the localization of Ubp5 to the bud neck and incipient bud sites.

Importantly, replacement of the N-terminal domain of Ubp5 with the LEL signal of Doa4 redirects the Ubp5 enzyme to the late endosome, and this chimera can partially suppress the phenotype of a *doa4*-null mutant. This indicates that the Ubp5 catalytic domain retains a substantial ability to function at the endosome on what are normally Doa4 substrates. The release of Ubp5 from bud neck–binding sites is not by itself sufficient to allow Ubp5 to function in place of Doa4. This inference is derived from the fact that $Ubp5_{\Delta 2–162}$-GFP, which no longer concentrates at the bud neck (Fig. 7 A), does not localize to the late endosome and is not able to suppress *doa4Δ* (not depicted). Collectively, these results indicate that proper Doa4 regulation requires Doa4 recruitment to the late endosome/MVB via its N-terminal LEL domain.

Suppression of *doa4* defects by the $Doa4_{LEL}$-Ubp5 chimera is not complete. Our previous experiments revealed that sequence differences between the rhodanese homology domain (RHD) of Doa4 (residues 199–322) and Ubp5 (148–277) are also important for full Doa4 function (Papa et al., 1999). This is confirmed in Fig. 6 C (compare sector 2 with 3). The exact functions of the RHD in these two enzymes are not known. Neither RHD has the catalytic site for rhodanese enzymatic activity; the RHD may function as a ubiquitin-binding domain or in substrate binding more generally.

The previous study of DUB localization most directly relevant to ours is that of Lin et al. (2000), which described the differential localization of two isoforms of a testis-specific UBP generated by alternative splicing. One isoform localizes to the nucleus in developing spermatids, whereas the other is extranuclear. The isoforms differ only in their N-terminal extensions. When the two N-terminal domains were fused to GFP and expressed in transiently transfected COS-7 cells, the fusions continued to show distinct subcellular localization, although the difference was not absolute. The functional significance of the different cellular distributions of the testis UBP isoforms was not examined.

There are some reports of specific subcellular sites of concentration for individual DUBs, but it was not possible in either of these earlier studies to verify the physiological requirement for such localization (Murray et al., 2004; Soboleva et al., 2005). Among the yeast DUBs, one enzyme, Ubp16, is exclusively membrane associated (Kinner and Kölling, 2003). Ubp16 localizes to the outer mitochondrial membrane via an alanine-rich stretch of amino acids close to its N terminus. This motif might function as a membrane anchor. However, the importance of the mitochondrial localization of Ubp16 is unclear. Neither ubiquitin-dependent proteolysis nor mitochondrial function was detectably altered by loss of the DUB (Kinner and Kölling, 2003).

Ubp5: a regulator of cytokinesis?

Cytokinesis in animal and fungal cells occurs through contraction of an actomyosin ring and subsequent abscission of a narrow intercellular bridge (Wolfe and Gould, 2005). In *S. cerevisiae*, several bud neck–localized proteins, including Hof1, are required for efficient cell separation. Interestingly, the degradation of Hof1 is required for efficient actomyosin ring contraction and cell separation (Blondel et al., 2005). The cellular concentration of Hof1 peaks in cells with large buds and dramatically drops during cytokinesis. The SCF^{Grr1} ubiquitin ligase colocalizes with Hof1 at the bud neck and mediates Hof1 degradation after activation of the mitotic exit network. We have found that Ubp5, like Hof1, concentrates at incipient bud sites and at the bud neck, although we do not yet know what cellular factors are required for this localization. Ubp5 may remove ubiquitin chains from Hof1, thereby rescuing Hof1 from premature degradation. Consistent with this idea, two-hybrid interactions have been detected between Ubp5 and Hof1 (Ito et al., 2001).

Binding of the Doa4 LEL domain to the late endosome

How might boxes A–D in the Doa4 LEL domain function in endosomal targeting? The sequences of the Doa4 and Ubp5 paralogues are sufficiently similar in their N-terminal domains to infer that the general fold of these regions is likely to be similar as well. Despite this, Ubp5, with its more diverged box A–D sequences, does not localize to the late endosome. Therefore, we imagine that these conserved motifs in Doa4 are at least partly exposed at the protein surface and mediate specific protein–protein or protein–membrane interactions that are necessary for late endosome binding. All four elements include multiple hydrophobic residues with interspersed charged or hydrophilic amino acids, which would be consistent with such a function.

Cell extraction in the absence of detergents suggests that ~40% of Doa4 is membrane bound in wild-type cells (unpublished data). Because Doa4 lacks any obvious transmembrane segments, it presumably associates peripherally with the late endosome/MVB membrane. Such an association could be mediated by a protein receptor, specific lipids, or both. We previously found that inactivation of the ESCRT-III components Snf7 or Vps24 prevents the localization of Doa4 to the class E compartment, indicating that Doa4 may interact directly or indirectly with subunits of this complex (Amerik et al., 2000b).

A genetic screen identified Doa4 as a high copy suppressor of a specific mutant *bro1* strain, and subsequent analysis suggested that the Bro1 class E VPS factor can bind to Doa4 and is necessary for recruitment of the DUB to the late endosome (Luhtala and Odorizzi, 2004). Consistent with this model, we have shown that ubiquitin profiles of *bro1Δ* and *doa4Δ* mutants are very similar, and earlier genetic analysis had also suggested that Bro1 could function before or together with Doa4 in the MVB pathway (Nikko et al., 2003). Surprisingly, we continue to see Doa4 concentrated in the class E compartment of *vps4Δ bro1Δ* cells, indicating that the Bro1 cofactor must do more than simply recruit Doa4 to the endosome. Bro1 binds directly via its so-called Bro1 domain to the Snf7 subunit of ESCRT-III (Kim et al., 2005). Therefore, Bro1 could function as a bridge between the ESCRT-III complex and Doa4. To date, we have not detected binding between Doa4 and Bro1 or any ESCRT-III components by either yeast two-hybrid analysis or tandem affinity purification (unpublished data). However, Bowers et al. (2004) reported a weak two-hybrid interaction between Doa4 and Snf7, although they also did not detect a Bro1–Doa4 interaction.

The binding between Bro1 and Doa4 is evidently quite weak (or is dynamic) under most conditions, so additional interactions between Doa4 and ESCRT-III components might also help recruit the DUB to the late endosome. Another Bro1-domain protein in yeast, Rim20, also binds Snf7 but is not required for membrane trafficking to the vacuole, instead functioning in the activation of a transcription factor (Boysen and Mitchell, 2006). Nevertheless, Rim20 might function redundantly with Bro1 in Doa4 recruitment to the late endosome, which is a possibility we are testing.

Various proteomic affinity purifications by different groups have yielded other potential Doa4 interactors, but the significance of these interactions remains to be tested (see http://www.yeastgenome.org/). One intriguing potential binding partner is Avt1. This transmembrane protein is an amino acid transporter of the vacuole (Russnak et al., 2001), and it might be present in prevacuolar compartment membranes. Avt1 could conceivably have a second function as a Doa4 receptor in the late endosome.

Substrate specificity of Doa4

The basis of substrate specificity among the DUBs is still only poorly understood in most cases. For some DUBs, specificity

has been traced to a specific substrate interaction motif, such as in HAUSP (Li et al., 2002), whereas for others, the enzyme has a unique way of interacting with the polyubiquitin chain such that the chain can only be bound and disassembled if certain conditions are met (e.g., the chain has a free proximal end in the case of IsoT; Reyes-Turcu et al., 2006). Doa4 must act on a wide range of ubiquitin-conjugated substrates, so it is predicted to have broad specificity. Our data indicate that a major means of regulating Doa4 function is through controlled subcellular localization. Nevertheless, additional mechanisms are likely to regulate its activity. Activity of purified Doa4 protein is very low (Papa and Hochstrasser, 1993; Papa et al., 1999; and unpublished data). The enzyme might be activated by binding to components of the MVB machinery (such as Bro1), which is analogous to Ubp6 activation by binding to the 26S proteasome (Leggett et al., 2002). Catalytic activity of AMSH, a mammalian DUB of the MPN^+/JAMM subfamily that also functions in the endocytic pathway, is stimulated by binding a specific MVB-sorting factor (McCullough et al., 2006). Doa4 activity might also be increased by lipid binding. Alternatively, Doa4 could be more active against a specific subclass of ubiquitin-linked substrates such as membrane proteins or those bearing Lys63-ubiquitin chains. Additional studies will be needed to distinguish between these possibilities.

Materials and methods

Strains, antibodies, and genetic techniques

Yeast strains used in this study are listed in Table I. The *E. coli* strains used for recombinant DNA work were JM101 and TOP10. Yeast and bacterial media were prepared as described previously, and standard yeast and bacterial molecular genetic methods were used (Ausubel et al., 2002). Monoclonal mouse antibodies against ubiquitin, GFP, and the c-myc epitope were purchased from Covance. Polyclonal rabbit antibody against β-galactosidase was purchased from MP Biomedicals. Rabbit antibodies against CPS and Snf7 were gifts from D. Katzmann (Mayo Clinic, Rochester, MN). Antibody against Matα2 was described previously (Hochstrasser and Varshavsky, 1990).

Yeast strain and plasmid constructions

DOA4 boxes A and B were individually deleted by a two-step PCR-based approach (Amerik et al., 1997). A YCplac33 plasmid carrying a 6,149-bp KpnI–PstI yeast genomic fragment including the *DOA4* gene (pDOA4-8) was used as a template (Papa and Hochstrasser, 1993). Amplified DNA fragments were cloned into pGEM-T (Promega). The resultant plasmids were digested with AgeI and BglII (restriction sites had been introduced into the respective flanking PCR primers), and the mutant *doa4* DNA fragments were cloned into AgeI–BglII-digested pDOA4-GFP, a 2-μm plasmid encoding a functional fusion of Doa4 with enhanced GFP. All constructs were verified by DNA sequencing.

The chromosomal *BRO1* gene was inactivated by PCR-based gene deletion using the pFA6a-TRP1 plasmid (Longtine et al., 1998) as a PCR template to create a DNA fragment that directed replacement of the chromosomal *BRO1* ORF with the *TRP1* gene by homologous recombination in MHY606 diploid yeast cells. Trp^+ transformants were checked for the deletion allele by PCR. The heterozygous diploids were sporulated, and tetrads were dissected.

An analogous approach was used for constructing plasmids encoding GFP fusions with different portions of Doa4. pFA6a-GFP(S65T)-HIS3MX6 was used as a template (Longtine et al., 1998). GFP fusions were made after Doa4 residues 128, 190, 208, 232, and 560 by recombining in MHY501 yeast cells PCR-amplified *GFP-HIS3* DNA fragments that had sequence identity upstream of the indicated *DOA4* codons and downstream of the *DOA4* stop codon with a cotransformed YEplac195-DOA4 (*URA3*) plasmid. His^+ Ura^+ colonies were screened for recombinant plasmids by PCR, and the plasmids were recovered in *E. coli* and reintroduced into various yeast strains for localization studies.

Table I. **Yeast strains used in this study**

Strain	Genotype
MHY501	*MATα his3-Δ200 leu2-3,112 ura3-52 lys2-801 trp1-1*
MHY623	*MATα his3-Δ200 leu2-3,112 ura3-52 lys2-801 trp1-1 doa4-Δ1::LEU2*
MHY954	*MATα his3-Δ200 leu2-3,112 ura3-52 lys2-801 trp1-1 doa4-Δ1::leu2::TRP1*
MHY1942	*MATα his3-Δ200 leu2-3,112 ura3-52 lys2-801 trp1-1 DOA4-Myc9-his5+*
MHY1947	*MATα his3-Δ200 leu2-3,112 ura3-52 lys2-801 trp1-1 vps4-Δ1::TRP1 DOA4-Myc9-his5+*
MHY2443	*MATα his3-Δ200 leu2-3,112 ura3-52 lys2-801 trp1-1 vps4-Δ1::TRP1*
MHY2476	*MATα his3-Δ200 leu2-3,112 ura3-52 lys2-801 trp1-1 pep4-Δ1::HIS3 prb1-Δ1::KAN doa4-Δ1::LEU2*
MHY2718	*MATα his3-Δ200 leu2-3,112 ura3-52 lys2-801 trp1-1 bro1-Δ1::TRP1*
MHY2732	*MATα his3-Δ200 leu2-3,112 ura3-52 lys2-801 trp1-1 bro1-Δ1::TRP1 vps4-Δ1::HIS5*
SEY6210	*MATα his3-Δ200 leu2-3,112 ura3-52 lys2-801 trp1-Δ901 suc2-Δ9*
PJ69-4A	*MATa his3-Δ200 leu2-3,112 ura3-52 lys2-801 trp1-901 gal4Δ gal80Δ LYS2::GAL1-HIS3 GAL2-ADE2 met2:GAL7-lacZ*

To construct plasmids that expressed full-length Ubp5 or the $Doa4_{1–560}$-$Ubp5_{444–805}$ chimera as fusions with GFP, the respective DUB ORFs were PCR amplified from either yeast genomic DNA or a plasmid encoding an HA-tagged $Doa4_{1–560}$-$Ubp5_{444–805}$ chimera, which was described previously (Papa et al., 1999). PCR products were digested with BamHI and HindIII and were ligated into BamHI–HindIII-restricted pUG35 (*CEN/URA3*; Euroscarf). The $Doa4_{1–208}$-$Ubp5_{163–805}$ chimera was made by a PCR gap repair method that was developed previously (Papa et al., 1999). The pUG35-UBP5 plasmid was gapped by digestion with AflII and SphI, the desired *DOA4* segment was amplified by PCR, and the two DNA fragments were cotransformed into MHY501 yeast cells. Recombinant plasmids were recovered in bacteria and sequenced to verify that they had the expected exchange of *UBP5* and *DOA4* sequences.

Plasmids encoding $Ubp5_{Δ2–35}$- and $Ubp5_{Δ2–162}$-GFP were constructed by a variation of the PCR gap repair method. pUG35-UBP5 was gapped with BamHI and AflII, and the large DNA fragment was isolated. Three oligonucleotides were designed as follows: an upstream 46-nucleotide primer was derived from the pUG35 sequence and included the start codon of the *UBP5* gene. The 5′ sequences of two downstream 65-mer oligonucleotides matched the noncoding strand of *UBP5* downstream of the codons for Pro35 and Ala162, respectively. Upstream and downstream pairs of primers had a 22-base overlap at their 3′ ends that straddled the deletion endpoints. The primers were annealed and extended with Taq DNA polymerase, resulting in an 89-bp double-stranded fragment that was introduced into yeast cells along with gapped pUG35-UBP5. Recombinant plasmids from Ura^+ colonies were recovered in *E. coli*, and the deletions were verified by DNA sequencing.

Pulse-chase and immunoblot analyses

Pulse-chase analysis of protein degradation was conducted as described previously (Chen et al., 1993). Cells were labeled for 5–10 min with [^{35}S]TransLabel (MP Biochemicals). SDS-PAGE gels were dried and analyzed using a Storm Phosphorimager and ImageQuant software (GE Healthcare).

Western immunoblot analyses were performed as described previously (Amerik et al., 1997). For antiubiquitin immunoblotting, cells were grown at 30°C to midlogarithmic phase and lysed in SDS gel loading buffer by heating to 100°C for 10 min; cleared supernatants were loaded onto 16% tricine polyacrylamide gels, and proteins were transferred to Immobilon-P membranes (Millipore). Membranes were boiled for 30 min in water before incubation with antiubiquitin antibody. Antibody binding was detected using ECL reagents (GE Healthcare). For anti-GFP and -CPS immunoblot analysis, cell extracts were prepared by lysis with 0.2 M NaOH and 0.2% mercaptoethanol for 10 min on ice (Volland et al., 1994). Trichloroacetic acid was added to a final concentration of 5%, and the samples were incubated for an additional 10 min on ice.

Precipitated proteins were collected by centrifugation, neutralized, dissolved in loading buffer, loaded onto 10% SDS-polyacrylamide gels, and analyzed by immunoblotting.

Fluorescence microscopy

Cellular distributions of Doa4 and Snf7 were examined in fixed yeast cells by indirect immunofluorescence as described previously (Amerik et al., 2000b). After overnight incubation with primary antibodies, cells were washed and incubated for 1 h with secondary antibodies (Oregon green anti–mouse and Texas red anti–rabbit IgG conjugates; Invitrogen). GFP and FM 4-64 fluorescence in live cells was imaged as described previously (Amerik et al., 2000b). Samples were viewed on a fluorescence microscope (Axioscope; Carl Zeiss MicroImaging, Inc.) with a plan-Apochromat 100× NA 1.4 objective lens equipped with a CCD camera (Axiocam; Carl Zeiss MicroImaging, Inc.). Images were processed using Openlab software (version 3.1.5; Improvision). All experiments were conducted at room temperature.

Online supplemental material

Fig. S1 shows the colocalization of Doa4- and Doa4$_{1–208}$-GFP with the vital dye FM 4-64 to the class E compartment in *vps4Δ* cells. Fig. S2 demonstrates continued class E compartment localization of Doa4-GFP in *vps4Δ bro1Δ* cells costained with FM 4-64. Online supplemental material is available at http://www.jcb.org/cgi/content/full/jcb.200605134/DC1.

We thank Daria Khramtsova for help with several early experiments and Dave Katzmann for antibodies.

This work was supported by National Institutes of Health grant GM53756 to M. Hochstrasser and a National Cancer Institute Howard Temin Award (K01) to A. Amerik.

Submitted: 22 May 2006
Accepted: 31 October 2006

References

Amerik, A.Y., and M. Hochstrasser. 2004. Mechanism and function of deubiquitinating enzymes. *Biochim. Biophys. Acta*. 1695:189–207.

Amerik, A.Y., S. Swaminathan, B.A. Krantz, K.D. Wilkinson, and M. Hochstrasser. 1997. In vivo disassembly of free polyubiquitin chains by yeast Ubp14 modulates rates of protein degradation by the proteasome. *EMBO J.* 16:4826–4838.

Amerik, A.Y., S.J. Li, and M. Hochstrasser. 2000a. Analysis of the deubiquitinating enzymes of the yeast *Saccharomyces cerevisiae*. *Biol. Chem.* 381:981–992.

Amerik, A.Y., J. Nowak, S. Swaminathan, and M. Hochstrasser. 2000b. The Doa4 deubiquitinating enzyme is functionally linked to the vacuolar protein-sorting and endocytic pathways. *Mol. Biol. Cell*. 11:3365–3380.

Ausubel, F.M., R. Brent, R.E. Kingston, D.D. Moore, J.G. Seidman, J.A. Smith, and K. Struhl, editors. 2002. Short Protocols in Molecular Biology: a Compendium of Methods from Current Protocols in Molecular Biology. Fifth edition. John Wiley and Sons Inc., New York.

Babst, M., B. Wendland, E.J. Estepa, and S.D. Emr. 1998. The Vps4p AAA ATPase regulates membrane association of a Vps protein complex required for normal endosome function. *EMBO J.* 17:2982–2993.

Babst, M., D.J. Katzmann, E.J. Estepa-Sabal, T. Meerloo, and S.D. Emr. 2002. ESCRT-III: an endosome-associated heterooligomeric protein complex required for mvb sorting. *Dev. Cell*. 3:271–282.

Blondel, M., S. Bach, S. Bamps, J. Dobbelaere, P. Wiget, C. Longaretti, Y. Barral, L. Meijer, and M. Peter. 2005. Degradation of Hof1 by SCF (Grr1) is important for actomyosin contraction during cytokinesis in yeast. *EMBO J.* 24:1440–1452.

Bowers, K., J. Lottridge, S.B. Helliwell, L.M. Goldthwaite, J.P. Luzio, and T.H. Stevens. 2004. Protein-protein interactions of ESCRT complexes in the yeast *Saccharomyces cerevisiae*. *Traffic*. 5:194–210.

Boysen, J.H., and A.P. Mitchell. 2006. Control of Bro1-domain protein Rim20 localization by external pH, ESCRT machinery, and the *Saccharomyces cerevisiae* Rim101 pathway. *Mol. Biol. Cell*. 17:1344–1353.

Chen, P., P. Johnson, T. Sommer, S. Jentsch, and M. Hochstrasser. 1993. Multiple ubiquitin-conjugating enzymes participate in the in vivo degradation of the yeast MATα2 repressor. *Cell*. 74:357–369.

Dupre, S., C. Volland, and R. Haguenauer-Tsapis. 2001. Membrane transport: ubiquitylation in endosomal sorting. *Curr. Biol.* 11:R932–R934.

Galan, J., and R. Haguenauer-Tsapis. 1997. Ubiquitin Lys63 is involved in ubiquitination of a yeast plasma membrane protein. *EMBO J.* 16:5847–5854.

Hershko, A., and A. Ciechanover. 1998. The ubiquitin system. *Annu. Rev. Biochem.* 67:425–479.

Hicke, L., and R. Dunn. 2003. Regulation of membrane protein transport by ubiquitin and ubiquitin-binding proteins. *Annu. Rev. Cell Dev. Biol.* 19:141–172.

Hochstrasser, M. 1996. Ubiquitin-dependent protein degradation. *Annu. Rev. Genet.* 30:405–439.

Hochstrasser, M., and A. Varshavsky. 1990. In vivo degradation of a transcriptional regulator: the yeast alpha 2 repressor. *Cell*. 61:697–708.

Hu, M., P. Li, M. Li, W. Li, T. Yao, J.W. Wu, W. Gu, R.E. Cohen, and Y. Shi. 2002. Crystal structure of a UBP-family deubiquitinating enzyme in isolation and in complex with ubiquitin aldehyde. *Cell*. 111:1041–1054.

Ito, T., T. Chiba, R. Ozawa, M. Yoshida, M. Hattori, and Y. Sakaki. 2001. A comprehensive two-hybrid analysis to explore the yeast protein interactome. *Proc. Natl. Acad. Sci. USA*. 98:4569–4574.

Katzmann, D.J., M. Babst, and S.D. Emr. 2001. Ubiquitin-dependent sorting into the multivesicular body pathway requires the function of a conserved endosomal protein sorting complex, ESCRT-I. *Cell*. 106:145–155.

Katzmann, D.J., G. Odorizzi, and S.D. Emr. 2002. Receptor downregulation and multivesicular-body sorting. *Nat. Rev. Mol. Cell Biol.* 3:893–905.

Kim, J., S. Sitaraman, A. Hierro, B.M. Beach, G. Odorizzi, and J.H. Hurley. 2005. Structural basis for endosomal targeting by the Bro1 domain. *Dev. Cell*. 8:937–947.

Kinner, A., and R. Kölling. 2003. The yeast deubiquitinating enzyme Ubp16 is anchored to the outer mitochondrial membrane. *FEBS Lett.* 549:135–140.

Leggett, D.S., J. Hanna, A. Borodovsky, B. Crosas, M. Schmidt, R.T. Baker, T. Walz, H. Ploegh, and D. Finley. 2002. Multiple associated proteins regulate proteasome structure and function. *Mol. Cell*. 10:495–507.

Li, M., D. Chen, A. Shiloh, J. Luo, A.Y. Nikolaev, J. Qin, and W. Gu. 2002. Deubiquitination of p53 by HAUSP is an important pathway for p53 stabilization. *Nature*. 416:648–653.

Lin, H., A. Keriel, C.R. Morales, N. Bedard, Q. Zhao, P. Hingamp, S. Lefrancois, L. Combaret, and S.S. Wing. 2000. Divergent N-terminal sequences target an inducible testis deubiquitinating enzyme to distinct subcellular structures. *Mol. Cell. Biol.* 20:6568–6578.

Longtine, M.S., A. McKenzie III, D.J. Demarini, N.G. Shah, A. Wach, A. Brachat, P. Philippsen, and J.R. Pringle. 1998. Additional modules for versatile and economical PCR-based gene deletion and modification in *Saccharomyces cerevisiae*. *Yeast*. 14:953–961.

Luhtala, N., and G. Odorizzi. 2004. Bro1 coordinates deubiquitination in the multivesicular body pathway by recruiting Doa4 to endosomes. *J. Cell Biol.* 166:717–729.

McCullough, J., P.E. Row, O. Lorenzo, M. Doherty, R. Beynon, M.J. Clague, and S. Urbe. 2006. Activation of the endosome-associated ubiquitin isopeptidase AMSH by STAM, a component of the multivesicular body-sorting machinery. *Curr. Biol.* 16:160–165.

Murray, R.Z., L.A. Jolly, and S.A. Wood. 2004. The FAM deubiquitylating enzyme localizes to multiple points of protein trafficking in epithelia, where it associates with E-cadherin and beta-catenin. *Mol. Biol. Cell*. 15:1591–1599.

Nijman, S.M., M.P. Luna-Vargas, A. Velds, T.R. Brummelkamp, A.M. Dirac, T.K. Sixma, and R. Bernards. 2005. A genomic and functional inventory of deubiquitinating enzymes. *Cell*. 123:773–786.

Nikko, E., A.M. Marini, and B. Andre. 2003. Permease recycling and ubiquitination status reveal a particular role for Bro1 in the multivesicular body pathway. *J. Biol. Chem.* 278:50732–50743.

Odorizzi, G., D.J. Katzmann, M. Babst, A. Audhya, and S.D. Emr. 2003. Bro1 is an endosome-associated protein that functions in the MVB pathway in *Saccharomyces cerevisiae*. *J. Cell Sci.* 116:1893–1903.

Papa, F., and M. Hochstrasser. 1993. The yeast *DOA4* gene encodes a deubiquitinating enzyme related to a product of the human *tre-2* oncogene. *Nature*. 366:313–319.

Papa, F.R., A.Y. Amerik, and M. Hochstrasser. 1999. Interaction of the Doa4 deubiquitinating enzyme with the yeast 26S proteasome. *Mol. Biol. Cell*. 10:741–756.

Reyes-Turcu, F.E., J.R. Horton, J.E. Mullally, A. Heroux, X. Cheng, and K.D. Wilkinson. 2006. The ubiquitin binding domain ZnF UBP recognizes the C-terminal diglycine motif of unanchored ubiquitin. *Cell*. 124:1197–1208.

Rieder, S.E., L.M. Banta, K. Kohrer, J.M. McCaffery, and S.D. Emr. 1996. Multilamellar endosome-like compartment accumulates in the yeast vps28 vacuolar protein sorting mutant. *Mol. Biol. Cell*. 7:985–999.

Russnak, R., D. Konczal, and S.L. McIntire. 2001. A family of yeast proteins mediating bidirectional vacuolar amino acid transport. *J. Biol. Chem.* 276:23849–23857.

Soboleva, T.A., D.A. Jans, M. Johnson-Saliba, and R.T. Baker. 2005. Nuclear-cytoplasmic shuttling of the oncogenic mouse UNP/USP4 deubiquitylating enzyme. *J. Biol. Chem.* 280:745–752.

Spormann, D.O., J. Heim, and D.H. Wolf. 1992. Biogenesis of the yeast vacuole (lysosome). The precursor forms of the soluble hydrolase carboxypeptidase yscS are associated with the vacuolar membrane. *J. Biol. Chem.* 267:8021–8029.

Swaminathan, S., A.Y. Amerik, and M. Hochstrasser. 1999. The Doa4 deubiquitinating enzyme is required for ubiquitin homeostasis in yeast. *Mol. Biol. Cell*. 10:2583–2594.

Verma, R., L. Aravind, R. Oania, W.H. McDonald, J.R. Yates III, E.V. Koonin, and R.J. Deshaies. 2002. Role of Rpn11 metalloprotease in deubiquitination and degradation by the 26S proteasome. *Science*. 298:611–615.

Volland, C., D. Urban-Grimal, G. Geraud, and R. Haguenauer-Tsapis. 1994. Endocytosis and degradation of the yeast uracil permease under adverse conditions. *J. Biol. Chem.* 269:9833–9841.

Weissman, A.M. 2001. Themes and variations on ubiquitylation. *Nat. Rev. Mol. Cell Biol.* 2:169–178.

Wilkinson, K.D., V.L. Tashayev, L.B. O'Connor, C.N. Larsen, E. Kasperek, and C.M. Pickart. 1995. Metabolism of the polyubiquitin degradation signal: structure, mechanism, and role of isopeptidase T. *Biochemistry*. 34:14535–14546.

Wolfe, B.A., and K.L. Gould. 2005. Split decisions: coordinating cytokinesis in yeast. *Trends Cell Biol.* 15:10–18.

Yao, T., and R.E. Cohen. 2002. A cryptic protease couples deubiquitination and degradation by the proteasome. *Nature*. 419:403–407.